Laser and Particle Beams (2009), *27*, 569–577.

doi:10.1017/S0263034609990279

Soft X-ray emissions from neon gas-puff Z-pinch powered by Qiang Guang-I accelerator

B. KUAI,[1,3] G. WU,[2,3] A. QIU,[1,3] L. WANG,[3] P. CONG,[3] AND X. WANG[4]

[1]Department of Electrical Engineering, Xi'an Jiaotong University, Xi'an, China
[2]Department of Engineering Physics, Tsinghua University, Beijing, China
[3]Northwest Institute of Nuclear Technology, Xi'an, China
[4]Department of Electrical Engineering, Tsinghua University, Beijing, China

(RECEIVED 26 March 2009; ACCEPTED 18 June 2009)

Abstract

The X-ray emission, especially the K-shell emission, from a neon gas-puff Z-pinch powered by the Qiang Guang-I accelerator, about 1.5 MA in amplitude and 100 ns in rise time, were calculated based on the two-level model and measured with X-ray diodes and an eight-frame X-ray pinhole camera. The simulation results showed that the K-shell yield is highly sensitive to the peak current. The experimental results confirmed that the matching of the Z-pinch load (mass and initial radius) to the current is crucial for getting a higher X-ray yield. Being determined by the imploding time, the pinch current plays a more important role than the current amplitude in K-shell emission. It seems that the preferable imploding time is about 110 ns. The K-shell radiation power with double shells, as a whole, is higher than that using single neon shell. While an implosion of a light (32 μg/cm) and small (20 mm in diameter) neon shell evolves with rather twist and asymmetries, a heavier (41 μg/cm) and bigger (25 mm in diameter) neon shell implodes more symmetrically. The double neon shells, 30 mm and 30 μg/cm for the outer shell, and 15-mm and 10 μg/cm for the inner shell, create almost "perfect" implosions evidenced by the early-time plasma shells with little perturbation and late stagnated pinch liners with a good axial uniformity. It was found that the "Zippering" effect leads to an earlier K-shell emission in the cathode region than that in the anode region, which extends the pulse width of K-shell emission.

Keywords: Gas puff z-pinch; Pulse power generator; Pulsed X-ray source; Z-pinch

1. INTRODUCTION

Pulsed and intense X-ray sources could be obtained from Z-pinch (Spielman, 2001), X-pinch (Liu *et al.*, 2008*a*, 2008*b*; Zou *et al.*, 2006), and laser-produced plasmas (Hong *et al.*, 2009; Rafique *et al.*, 2008; Abdallah *et al.*, 2007; Schollmeier *et al.*, 2006). For X-pinch X-ray sources, they were produced by pulsed discharge of high current and usually used as point sources for backlighting high-density plasmas or for phase-contrast imaging of biological objects. For the X-ray sources from laser-produced plasmas, they were produced by the bombardment of pulsed and intense laser on the targets, and usually used as probing X-rays. Being different from the X-pinch plasma and laser-produced plasma, the hot plasma produced by gas puff or wire array Z-pinches is one of the most efficient X-ray sources in laboratories (Libermann *et al.*, 1999; Ryutov *et al.*, 2000). About 20% of the primary electric energy of the generators can be converted into soft X-ray emission (Deeney *et al.*, 1997; Sanford *et al.*, 1996). Numerous pulsed power machines over the last 35 years have pursued the use of Z-pinch loads as sources of radiation. Load designs have included gas puffs and wire arrays, with emissions from the K-shell of the materials with low to moderate atomic number (neon ~1.0 keV, aluminum ~1.7 keV, argon ~3 keV, titanium ~4.8 keV, and iron ~6.7 keV) all being studied (Coverdale *et al.*, 2000; Chaikovsky *et al.*, 2003). These loads were designed to offer the environments mainly for testing the effects of the pulsed intense X-ray radiation and the material studies. Being capable of delivering to Z-pinch loads a pulsed current of 1.5 MA in amplitude and 100 ns in rise time, Qiang Guang-I generator is the main facility in China for the experimental research on high power Z-pinches. Tens of kilo-joule soft X-rays could be obtained on it, when using

Address correspondence and reprint requests to: X. Wang, Department of Electrical Engineering, Tsinghua University, Beijing 100084, China. E-mail: wangxx@mail.tsinghua.edu.cn. Or to A. Qiu, Northwest Institute of Nuclear Technology, Xi'an, China. E-mail: qiuac@cae.cn

krypton gas puff (Kuai *et al.*, 2002) or tungsten wire array loads (Qiu *et al.*, 2006). In this paper, we present the theoretical and experimental results of a neon Z-pinch with the gas-puff loads produced using the annular, single and double-shell supersonic nozzles of 2 and 3-cm diameters.

2. K-SHELL RADIATION FROM SIMULATION

In order to get an efficient K shell emission, the mass and radius of a Z-pinch load should be matched to the amplitude and rise time of the current output from the generator (Commisso *et al.*, 1998). For striping and heating a neon atom to its K shell, it requires a minimum energy, $E_{\min}$, about 5.4 keV per ion. Assuming that the primary energy input to the plasma is kinetic energy, the final kinetic energy per ion, E_{ion}, should be in excess of $E_{\min}$ for an effective radiation from the K-shell. A dimensionless parameter η is defined by $\eta = E_{ion}/E_{\min}$ for convenience (Whitney *et al.*, 1990). A criterion $\eta > 2$ was usually considered for getting a significant K-shell yield, i.e., $E_{ion} > 10.8eV/ion$, which corresponds to the kinetic energy per centimeter $E_{kinetic} > 1kJ/cm$ for a representative load with a line mass density, m, of 20 μg/cm.

According to the 0-D slug model, $E_{kinetic}$ may be expressed as

$$E_{kinetic} = \gamma \ln\left(\frac{R_0}{R_f}\right) I_0^2, \tag{1}$$

where I_0 is the peak current, in unit of MA; $\gamma < 1$ is a factor that accounts for the fact that the average current during implosion is less than I_0; R_0, and R_f are the initial radius and the final radius of the plasma column, respectively. For $\gamma \sim 0.8$ and a compression ratio $R_0/R_f \sim 10$, $E_{kinetic}$ is in the range of 3 kJ/cm to 6 kJ/cm corresponding to the peak current varying from 1.3 MA to 1.8 MA from Qiang Guang-I accelerator. This means that the line mass density of the neon gas puff load powered by Qiang Guang-I accelerator can be varied in the range of 10–100 μg/cm.

A two-level model for K-shell radiation scaling of Z-pinch was developed (Mosher *et al.*, 1998). The model is very useful in the prediction of the K-shell X-ray yields from Z-pinch radiation source as a function of the load parameters and the results had been shown to agree with the neon gas-puff experiments at 0.7 MA and the aluminum wire-array experiments at 7 MA. According to this model, the yield of K-shell radiation, Y, for a stagnated-plasma column with a uniform density could be related with an optically thin radiation yield, Y_{thin}, by an escape fraction, *i.e.*, $Y = C_{escape} \cdot Y_{thin}$.

$$Y_{\text{thin}} = \frac{39 \cdot m^2}{R_f \cdot T \cdot Z_A^{1.2}} \exp\left(-\frac{10.2 Z_A^2}{T}\right), \tag{2}$$

where Y_{thin} is in unit of kJ/cm; C_{escape} is the escape fraction determined by the optical depth and R_f; R_f is the final radius of the pinched plasma column in unit of cm; m is the line mass density of the load in unit of μg/cm; T is the temperature of the stagnated-plasma in unit of eV; Z_A is the atomic number of the load material.

By considering the energy-balance and introducing a simple equation

$$E_{kinetic}/2 = E_{internal} + Y, \tag{3}$$

where $E_{internal}$ is the internal energy of the plasma in unit of kJ/cm and can be calculated with the following formula

$$E_{internal} = 1.8 \times 10^{-4} m \cdot T / Z_A^{0.28}, \tag{4}$$

one can numerically solve the equations of the two-level system and determine the X-ray yield.

This model was applied to predict the radiation performance of the neon gas-puff loads imploded on Qiang Guang-I. On the assumptions of $\gamma = 0.8$ and $R_0/R_f = 10$, the K-shell yield and the temperature of the stagnated-plasma as functions of the line mass density and the final radius of a 4-cm long plasma column as well as the current were obtained, as shown in Figure 1.

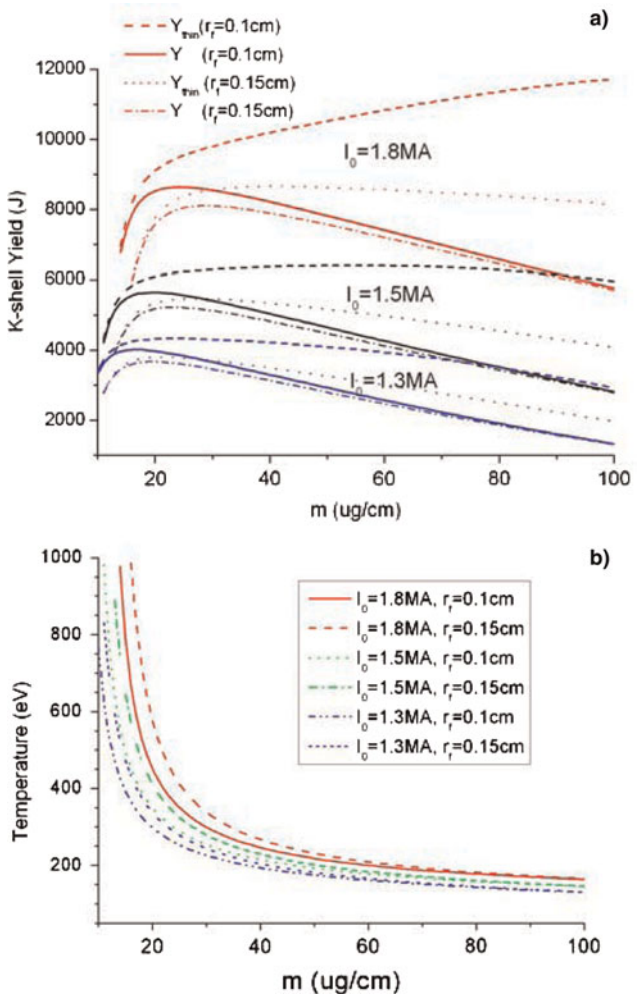

Fig. 1. (Color online) K-shell yield (**a**) and plasma temperature (**b**) as functions of the line mass density and the final radius of the plasma column as well as the current.

https://doi.org/10.1017/S0263034609990279 Published online by Cambridge University Press

It is easy to understand that the K-shell yield is highly sensitive to the peak current, since the main energy source is assumed to be the kinetic energy, hence proportional to the peak current. A load with a line mass density of about 20 μg/cm driven by 1.8 MA peak current may produce maximum yield up to ~8.5 kJ. For heavier masses, the plasma temperature decreases to a value below 200 eV, which results in K-shell radiation being reduced rapidly. Lower temperatures also correspond to a longer optical thickness, confirmed by an increasing gap between the total yield Y and optical thin yield Y_{thin}. If the load mass is too low, plasmas will become too hot, also leading to a reduced K-shell yield. A load with a line mass density lower than 20 μg/cm will be heated to a temperature in excess of 600 eV and the neon ions should be fully stripped. In addition, a higher plasma temperature but a lower yield of K-shell radiation will be produced by a plasma column with a larger final pinch diameter (0.15 cm) in comparison to that by a thinner plasma column (0.1 cm), maybe due to the lower density corresponding to a larger column, which greatly reduces the radiation rate.

3. EXPERIMENTAL SETUP

3.1. Qiang Guang-I Generator

The schematic of Qiang Guang-I generator is shown in Figure 2. The first stage of the generator is a linear transformer device (LTD) consisting of 120 capacitors of 2.8 μF/50 kV and 60 gas spark switches that are grouped into 30 modules, each module has a common magnetic core. As the succeeding stages of the generator, three water lines, a 1.4 Ω pulse forming line (PFL), a 0.75 Ω pulse compressing line (PCL), a pulse-transmitting line (PTL), are connected in series by a main switch and a multi-channel switch. Both switches operate in the self-breakdown mode. The Z-pinch chamber includes a magnetically insulated transmission line and a Z-pinch load. If the capacitors in LTD are charged to 42 kV, corresponding to a storage energy of 300 kJ, the generator can deliver a pulsed current, 2.3 MA in amplitude and 70 ns in rise time, to a short-circuit load of 40-nH inductance. Figure 3 is the typical waveform of the short-circuit current.

3.2. Neon Gas Puff Z-Pinch Load

Based on the simulation results mentioned in Section 2, the gas puff Z-pinch load was designed and sketched in Figure 4. A Laval nozzle inserted in the cathode was used for puffing out a supersonic neon shell into the vacuum space between the anode and the cathode as a Z-pinch load. The distance between the anode and the cathode was fixed at 40 mm. A "breakdown pin" was positioned behind the mesh anode and biased at a voltage of −300 V relative to the anode. When the gas puffed out from the cathode arriving at the mesh anode, a breakdown happens between the pin and the anode mesh, producing a voltage pulse as a signal to trigger the Qiang Guang-I generator.

For Z-pinch load, the line mass density, the mass per unit length between the anode and the cathode, is an important parameter that should be matched to the current from the pulsed generator. The line mass density of the gas shell from our Laval nozzle can be estimated using the following formula (Wang *et al.*, 2005):

$$m = 1.1p \cdot A \cdot S, \tag{5}$$

where m is the line mass density, in unit of μg/cm, p is the gas pressure, in units of 0.1 MPa; A is the atomic mass number of the gas, and S is the cross section area of the throat in the nozzle, in unit cm^2.

It was suggested that the double nested gas shells as a load would greatly enhance the power of X-ray radiation from Z-pinch (Deeney *et al.*, 1998). The double nested nozzle, sketched in Figure 5, was also designed and used in our experiments. As shown in Figures, 1 and 13 are the gas inlets; 2 and 11 are the plenum boxes; 3 is the solenoid coil for producing magnetic force to open the valves when a pulsed current flows through the coil; 4 is the pull rod; 5 is the striking block of iron; 6 is the spring for automatically resetting the position of the striking block, 7 is the spring for pressing the valves, 9 and 10 are the valves for puffing the outer and the inner gas

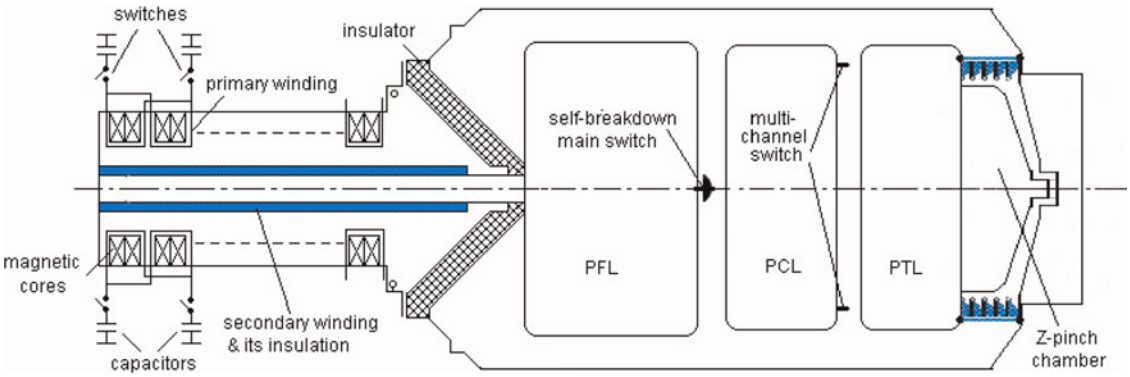

Fig. 2. (Color online) Schematic of Qiang Guang-I pulsed power facility.

https://doi.org/10.1017/S0263034609990279 Published online by Cambridge University Press

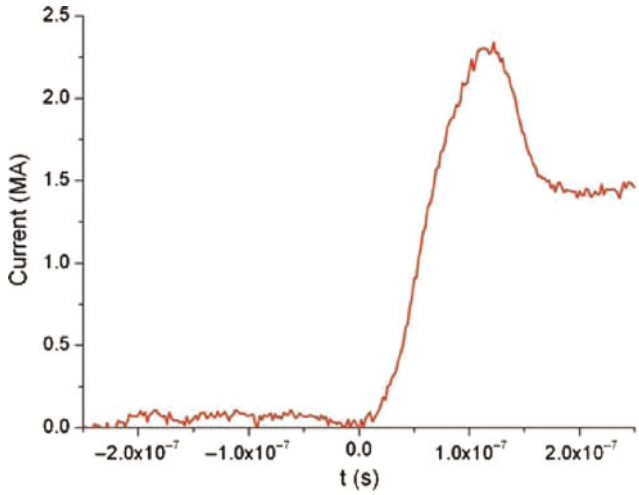

Fig. 3. (Color online) Typical waveform of the short-circuit current from Qiang-Guang-I generator.

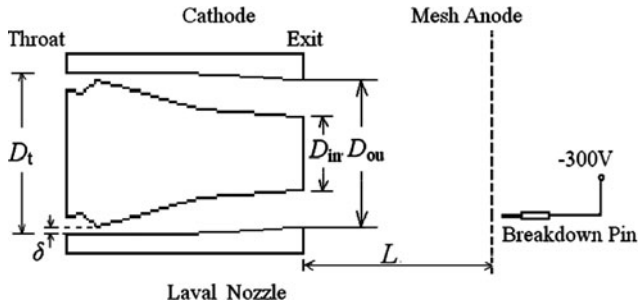

Fig. 4. Schematic of the configuration of gas puff Z-pinch load.

Table 1. *The parameters of the tested nozzles (unit: mm)*

Nozzle no.	Outer nozzle				Inner nozzle			
	D_t	δ	D_{out}	D_{in}	D_t	δ	D_{out}	D_{in}
1	22.3	0.25	20	11	—	—	—	—
2	28.5	0.25	25	14	—	—	—	—
3	35.7	0.36	30	24	11.8	0.49	10	7
4	43.6	0.32	30	28	15.7	0.31	15	11

shells, respectively; 12 is the wall of the inner chamber; 14 are the nozzles. We have tested four nozzles with the different parameters as were listed in Table 1. While nozzle 1 and 2 are used for producing a single gas shell, nozzle 3 and 4 serve as double nested gas shells.

3.3. Diagnostics

The load current was measured with a Rogowski coil installed on the anode disk at the radius of 22 cm. The power of K-shell (0.9–1.5 keV) radiation from the neon Z-pinch was measured using X-ray diodes (XRDs) with an aluminum cathode. Different filters were used and the corresponding sensitivities for the combinations of the filters and XRD were shown in Figure 6.

An eight-frame pinhole camera, with 2 ns time resolution, was used to take the pictures of the time-resolved X-ray emission from the neon Z-pinch. The eight frames were divided into two groups each consisting of four frames. The first group filtered by 1-μm thick Mylar is for the measurement of the emission in the broad spectrum (K-shell plus XUV),

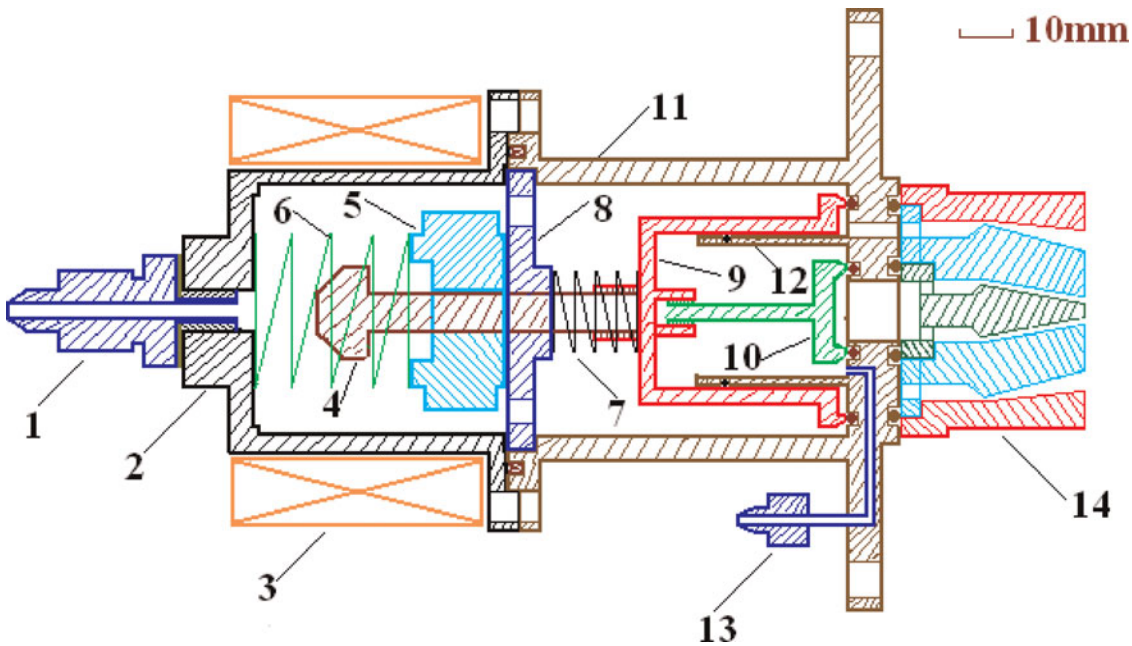

Fig. 5. (Color online) Double nested nozzles.

https://doi.org/10.1017/S0263034609990279 Published online by Cambridge University Press

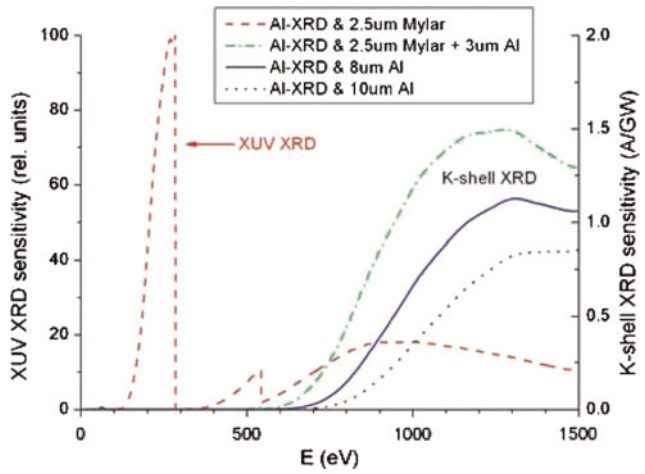

Fig. 6. (Color online) Sensitivities of the differently filtered XRDs.

the second group with an additional filter made of 8-μm thick aluminum foil for K-shell emission.

A four-frame gated spectrometer with TAP curved crystal was under developing to record the spectrum of K-shell lines for diagnosing plasma through the ratios of line intensity. Only a few spectrum data were recorded in late double-shell experiments.

4. RESULTS AND DISCUSSIONS

The typical results from the experiments with these four nozzles were listed in Table 2 and 3 in which the imploding time is defined as the time interval between the beginning of the current and the peak of K-shell X-ray power measured with the XRD. The X-ray energy was obtained by the integration of the K-shell X-ray power over the time.

Table 2 shows the experimental results for nozzles 1 and 2 that produce a single neon shell with an initial outer diameter of 20 mm and 25 mm, respectively. For nozzle 1, a higher X-ray output was obtained by using a higher current (~1.59 MA) combined with a heavier load (23 μg/cm–31 μg/cm) than that by using a little bit lower current (~1.38 MA) combined with a lighter load (12 μg/cm–19 μg/cm). However, for nozzle 2, too heavy or too light a load will considerably reduce the X-ray output. All of these may be explained with the imploding time, or more exactly speaking, with the pinch current, i.e., the current at the time when the plasma column is compressed to its smallest radius. As we know the X-ray yield is highly sensitive to the pinch current and the load should be matched to the current, otherwise the plasma may be under-heated or over-heated, leading to less K-shell X-ray output. It should be indicated that the current listed in Table 2 is the current amplitude

Table 2. *Typical results for single neon shell as Z-pinch load*

Nozzle no.	Shot no.	Current (MA)	Line mass density (μg/cm)	Imploding time (ns)	X-ray energy (kJ)	Radiation power (GW)
1	07059	1.53	31	107	4.0	93
	07061	1.59	27	103	5.0	112
	07056	1.59	23	109	5.6	132
	07069	1.37	19	91	2.8	68
	07070	1.38	16	92	2.0	44
	07071	1.38	12	95	2.5	54
2	07117	1.54	40	137	2.2	78
	07114	1.59	35	138	2.0	97
	07112	1.48	30	118	2.4	109
	07127	1.47	25	126	4.7	203
	07107	1.52	20	112	4.4	110
	07118	1.52	15	112	4.5	125
	07120	1.47	10	93	2.3	59

Table 3. *Typical results for double neon shells as Z-pinch load*

Nozzle no.	Shot no.	Current (MA)	Line mass density (μg/cm)	Imploding time (ns)	X-ray energy (kJ)	X-ray power (GW)
3	07131	1.66	67	142	1.56	54
	07143	1.72	42	150	1.97	65
	07140	1.64	33	134	4.71	178
	07139	1.58	25	119	4.87	216
	07137	1.70	21	137	5.58	256
	07133	1.65	17	135	5.59	211
4	08023	1.65	40	144	7.3	280
	08035	1.63	27	154	6.0	261

https://doi.org/10.1017/S0263034609990279 Published online by Cambridge University Press

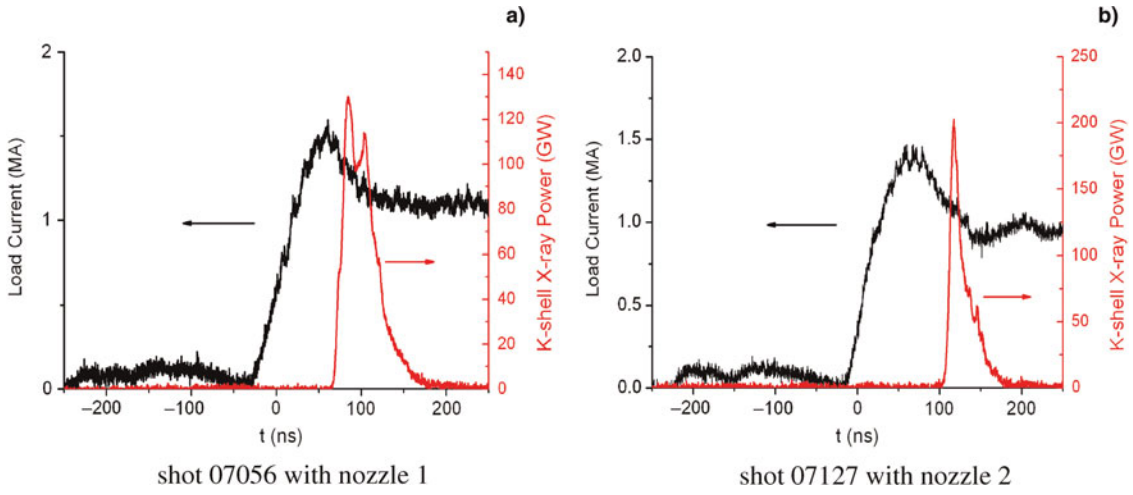

Fig. 7. (Color online) Time relationship between the load current and X-ray pulse.

Table 4. *Results for the six shots for which the X-ray pinhole images were shown in Figures 8–11*

Nozzle no.	Shot no.	Line mass density (μg/cm)	Current (MA)	Imploding Time (ns)	K-shell Yield (kJ)	K-shell Power (GW)	Pulse Width (ns)	Diameter of K-shell emitting region (mm)
1	07126	32	1.37	107	3.2	85	32	3.5
2	07179	41	1.57	140	3.1	130	14	2.1
3	08015	18 + 8	1.68	136	6.0	158	34	4.5
	08019	18 + 13	1.57	144	5.0	196	18	1.7
4	08023	30 + 10	1.65	144	7.3	280	25	2.2
	08035	20 + 7	1.63	154	6.0	261	22	2.0

rather than the pinch current. The pinch current could be determined with Figure 7 by considering the pinch current as the current at the time when the X-ray begins to burst. From Table 2 we could see that the imploding time increases with the increase of the line mass density. If the imploding time is too short for a lighter load or too long for a heavier load, the pinch current will be much smaller than the current amplitude, leading to a reduced K-shell X-ray output maybe due to the overheating or under-heating of the plasma. It seems that the preferable imploding time is about 110 ns for a current of about 1.5 MA in amplitude from Qiang Guang-I accelerator.

Table 3 shows the experimental results for nozzles 3 and 4 that produce double neon shells with the parameters listed in Table 1. Since the line mass density and the radius of the double neon shells were increased a little bit compared to that of the single neon shell, the current was correspondingly raised to ~1.65 MA from ~1.5 MA. The dependences of the X-ray output on the line mass density are more or less the same as using single neon shell, except that the K-shell radiation power with double shells, as a whole, is higher than that using single neon shell. The evolution of the X-ray sources from the neon gas puff Z-pinch was recorded with an eight-frame pinhole camera. The times marked on the pictures are relative to the power peak of K-shell emission and the cathode was at the right side of each picture. The pictures from 7 typical shots were chosen and the corresponding data were listed in Table 4.

Figure 8 shows four time-resolved pictures from shot 07162 for which the Z-pinch load is a single neon shell of 20 mm in the initial outer diameter and 32 μg/cm in line mass density. Since the load mass is low and the initial radius of the neon shell was small, the imploding time was only 107 ns, so short that the stagnated plasma column was

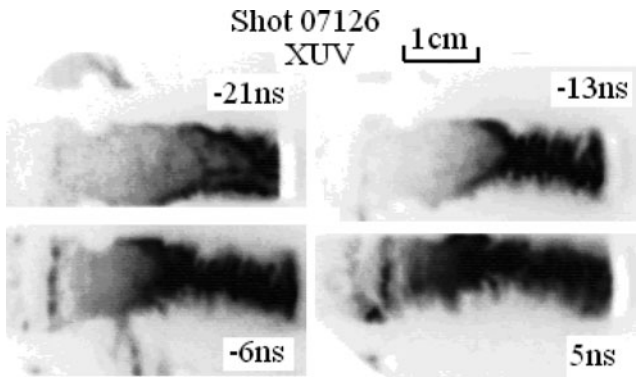

Fig. 8. Typical pinhole images of the X-ray emission from the Z-pinch load produced with nozzle 1.

https://doi.org/10.1017/S0263034609990279 Published online by Cambridge University Press

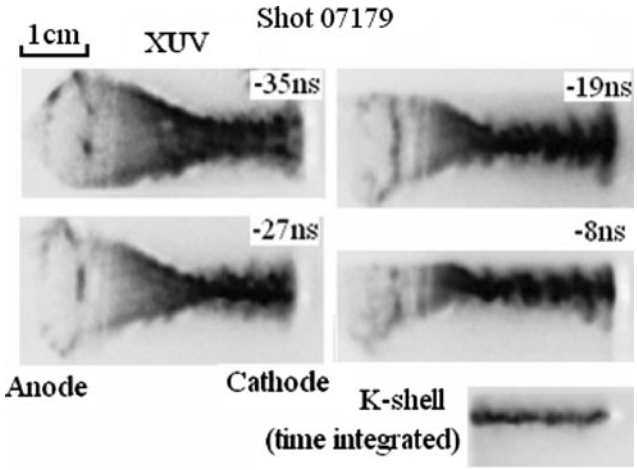

Fig. 9. Typical pinhole images of the X-ray emission from the Z-pinch load produced with nozzle 2.

strongly confined by and interacted with the magnetic field produced by the nearly peak current, hence evolved with rather twist and asymmetries. For shot 07179, the Z-pinch load is a single neon shell of 25 mm in the initial diameter and 41 μg/cm in line mass density, the plasma shell imploded more symmetrically, as shown in Figure 9, and with a relatively longer imploding time of 140 ns. A well-defined and tight pinch was formed which radiated in a single pulse of FWHM ∼15 ns. Comparison of the time-

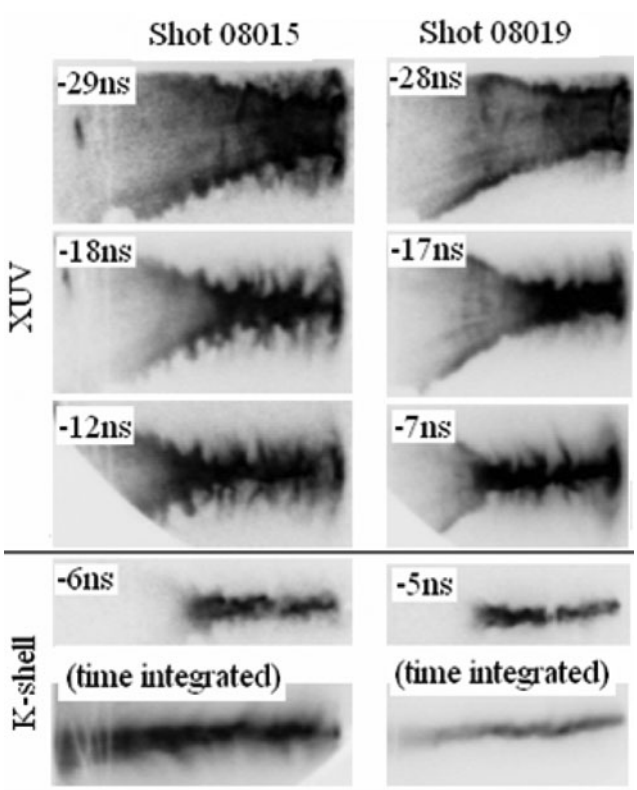

Fig. 10. Typical pinhole images of the X-ray emission from the Z-pinch load produced with nozzle 3.

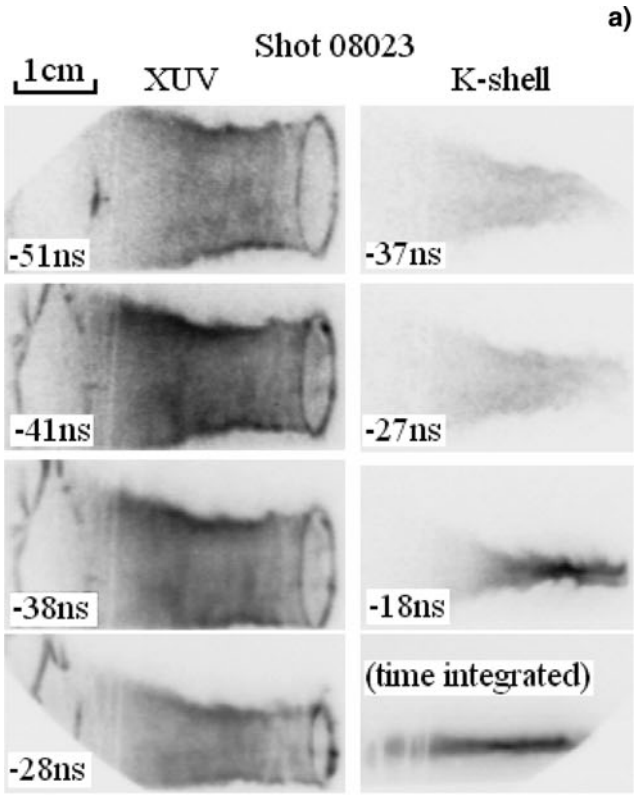

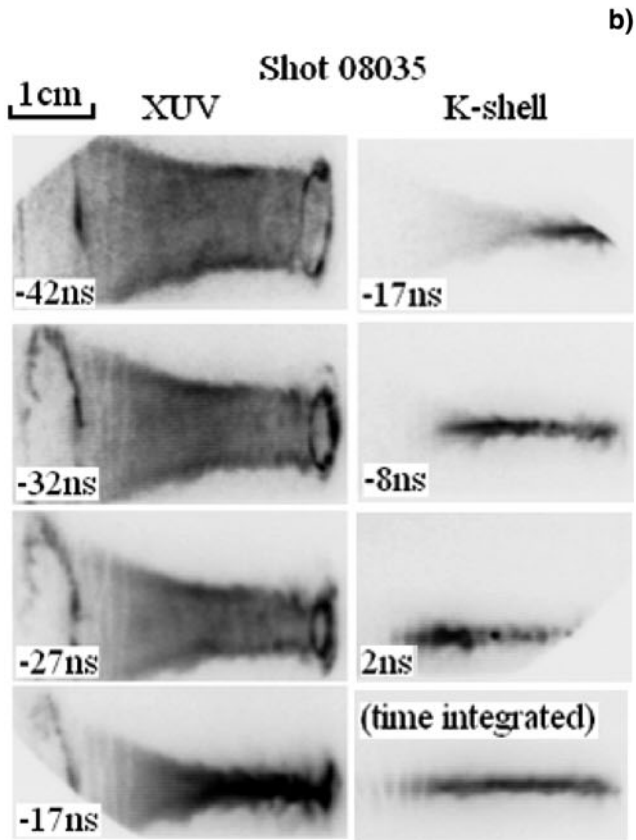

Fig. 11. Typical pinhole images of the X-ray emission from the Z-pinch load produced with nozzle 4.

https://doi.org/10.1017/S0263034609990279 Published online by Cambridge University Press

resolved XUV images with the time-integrated K-shell image indicates that only a part of the stagnated mass making contribution to K-shell emission. For nozzle 3 that produces double neon shells with the initial outer diameter of 30 mm and 10 mm, respectively, a low line mass density (17–30 μg/cm) is usually required to obtain high X-ray yield. It was found from the pictures of shot 08015 in Figure 10 that the hydrodynamic instabilities grew rapidly on the surface of plasma shell as the outer shell collided with a too light inner shell (8 μg/cm). The region of K-shell emission extended so much that the diameter of the time integrated image exceeded 4 mm. Once the inner shell got heavier (13 μg/cm), as shown in the pictures of shot 08019 in Figure 10, the surface instabilities seemed to be much depressed, leading to a more compact region (<2 mm) of K-shell emission.

The Z-pinch loads of double neon shells from nozzle 4 seems creating almost "perfect" implosions, as were evidenced by the early-time plasma shells with little perturbation (shot 08023 of Fig. 11) and late stagnated pinch liners with good axial uniformity (shot 08035 of Fig. 11). Time-resolved K-shell images show that even in the phase of snow-plow implosion (37 ns before the peak power) plasma had already been heated to the temperature of emitting K-shell X-ray. The K-shell emission in the region of the cathode starts about 20 ns earlier than that at the anode, indicating that the "Zippering" effect plays an important role in determining the pulse width of K-shell emission.

The spectrum of neon gas-puff Z-pinch with a load of the double shells was recorded using the spectrometer equipped with a TAP curved crystal and is shown in Figure 12. From the spectrum the K-shell lines of $L_{y-\alpha}$ from the hydrogen-like ions of neon and $H_{e-\alpha}$, $H_{e-\beta}$, and $H_{e-\gamma}$ from the helium-like ions of neon were clearly observed. As was expected, the resonant lines $L_{y-\alpha}$ and $H_{e-\alpha}$ are with higher intensity. The plasma parameters such as the electron density, the electron temperature as well as the ionizing state of the neon ions would be obtained based on the spectrum in the near future.

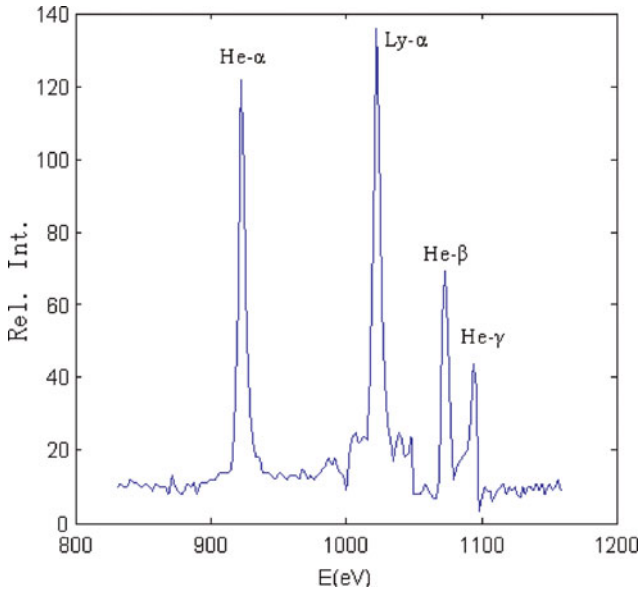

Fig. 12. (Color online) Typical spectrum of neon from the double shell gas puff Z-pinch.

5. CONCLUSIONS

The X-ray emissions, especially the K-shell emission, from a neon gas-puff Z-pinch powered by Qiang Guang-I accelerator, about 1.5 MA in amplitude and 100 ns in rise time, were calculated based on the two-level model and measured with X-ray diodes and an eight-frame X-ray pinhole camera. The simulation results showed that the K-shell yield is highly sensitive to the peak current. The experimental results confirmed that the matching of the Z-pinch load (mass and initial radius) to the current is crucial for getting a higher X-ray yield. Being determined by the imploding time, the pinch current plays a more important role than the current amplitude in K-shell emission. It seems that the preferable imploding time is about 110 ns. The K-shell radiation power with double shells, as a whole, is higher than using single neon shell. While an implosion of a light (32 μg/cm) and small (20 mm in diameter) neon shell evolves with rather twist and asymmetries, a heavier (41 μg/cm) and bigger (25 mm in diameter) neon shell implodes more symmetrically. The double neon shells, 30 mm and 30 μg/cm for the outer shell, and 15-mm and 10 μg/cm for the inner shell, create almost "perfect" implosions evidenced by the early-time plasma shells with little perturbation and late stagnated pinch liners with a good axial uniformity. It was found that the "Zippering" effect leads to an earlier K-shell emission in the cathode region than that in the anode region, which extends the pulse width of K-shell emission.

ACKNOWLEDGEMENTS

The authors would like to thank all our colleagues who worked on the Qiang Guang-I facility, especially to M.T. Qiu, T.S. Lei, T.P. Sun, N. Guo, T. Huang, J.J. Han, X.J. Zhang, G.W. Zhang, and K.L. Qiao for their contributions to the research. The authors would like also to thank the National Natural Science Foundation of China for supporting the research under contracts 10635050 and 50637010.

REFERENCES

Abdallah, J., Batani, D., Desai, T., Lucchini, G. Faenov, A., Pikuz, T., Magunov, A. & Narayanan, V. (2007). High resolution X-ray emission spectra from picosecond laser irradiated Ge targets. *Laser Part. Beams* **25**, 245–252.

Chaikovsky, S.A., Labetsky, A.Yu., Oreshkin, V.I., Shishlov, A.V., Baksht, R.B., Fedunin, A.V. & Rosskikh, A.G. (2003). The K-shell radiation of a double gas puff *z*-pinch with an axial magnetic field. *Laser Part. Beams* **21**, 255–264.

Commisso, R.J., Apruzese, J.P., Black, D.C., Boller, J.R., Moosman, B., Mosher, D., Stephanakis, S.J., Weber, B.V. & Young, F.C. (1998). Results of radius scaling experiments and

https://doi.org/10.1017/S0263034609990279 Published online by Cambridge University Press

analysis of Ne K-shell radiation data from an inductively driven Z-Pinch. *IEEE Trans. Plasma Sci.* **26**, 1068–1085.

Coverdale, C.A., Deeney, C., Douglas, M.R., Nailey, J., Whitney, K.G. Apruzese, J.P., Thornhill, J.W., Davis, J. & Schneider, R. (2000). Multi-keV photon production on the Z accelerator. *27th IEEE Intern. Conf. Plasma Sci.* 135.

Deeney, C., Nash, T.J., Spielman, R.B., Seaman, J.F., Chandler, G.C., Struve, K.W., Porter, J.L., Stygar, W.A., McGurn, J.S., Jobe, D.O., Gilliland, T.L., Torres, J.A., Vargas, M.F., Ruggles, L.E., Breeze, S., Mock, R.C., Douglas, M.R., Fehl, D.L., McDaniel, D.H. & Matzen, M.K. (1997). Power enhancement by increasing the initial array radius and wire number of tungsten Z pinches. *Phys. Rev. E* **56**, 5945–5958.

Deeney, C., Douglas, M.R., Spielman, R.B., Nash, T.J., Peterson, D.L., Eplattenier, P.L, Chandler, G.C., Seamen, J.F. & Struve, K.W. (1998). Enhancement of X-ray power from a z pinch using nested-wire Arrays. *Phys. Rev. Lett.* **81**, 4883–4886.

Hong, W., He, Y., Wen, T., Du, H., Teng, J., Qing, X., Huang, Z., Huang, W., Liu, H., Wang, X., Huang, X., Zh, Q., Ding, Y. & Peng, H. (2009). Spatial and temporal characteristics of X-ray emission from hot plasma driven by a relativistic femtosecond laser pulse, *Laser Part. Beams* **27**, 19–26.

Kuai, B., Cong, P., Zeng, Z., Qiu, A., Qiu, M., Chen, H., Liang, T., He, W., Wang, L. & Zhang, Z. (2002). An experimental study on Kr gas-puff Z-pinch. *Plasma Sci. Techn.* **4**, 1329–1333.

Libermann, M.A., DeGroot, J.S., Toor, A. & Spielman, R.B. (1999). *Physics of High-Density Z-Pinch Plasmas*, New York: Springer-Verlag.

Liu, R., Zou, R., Wang, X., He, L. & Zeng, N. (2008*a*). X-pinch experiments with pulsed power generator (PPG-1) at Tsinghua University. *Laser Part. Beams* **26**, 33–36.

Liu, R., Zou, R., Wang, X., Zeng, N. & He, L. (2008*b*). X-ray emission from an X-pinch and its applications. *Laser Part. Beams* **26**, 455–460.

Mosher, D., Qi, N. & Krishnan, M. (1998). A two-level model for K-shell radiation scaling of the imploding Z-pinch plasma radiation source. *IEEE Trans. Plasma Sci.* **26**, 1052–1061.

Qiu, A., Kuai, B., Zeng, Z., Wang, W., Qiu, M., Wang, L., Cong, P. & Lv, M. (2006). Study on W wire array *Z* pinch plasma radiation at Qiangguang-I facility. *Acta Phys. Sin.* **55**, 5917–5922.

Rafique, M., Khaleeq-Ur-Rahman, M., Riaz, I., Jalil, R. & Farid, N. (2008). External magnetic field effect on plume images and X-ray emission from a nanosecond laser produced plasma. *Laser Part. Beams* **26**, 217–224.

Ryutov, D.D., Derzon, M.S. & Matzen, M.K. (2000). The physics of fast Z-pinches. *Rev. Mod. Phys.* **72**, 167–223.

Sanford, T.W.L, Allshouse, G.O., Marder, B.M., Nash, T.J., Mock, R.C., Spielman, R.B., Seamen, J.F., McGurn, J.S., Jobe, D., Gilliland, T.L., Vargas, M., Struve, K.W., Stygar, W.A., Douglas, M.R. & Matzen, M.K. (1996). Improved symmetry greatly increases X-ray power from wire-array z-pinches. *Phys. Rev. Lett.* **77**, 5063–5066.

Schollmeier, M., Prieto, G., Rosmej, F.B., Schumann, G., Blazevic, A., Rosmej, O.N. & Roth, M. (2006). Investigation of laser-produced chlorine plasma radiation for non-monochromatic X-ray scattering experiments. *Laser Part. Beams* **24**, 335–345.

Spielman, R.B. (2001). Guest editor's preface: Z-pinch special issue. *Laser Part. Beams* **19**, 321–321.

Wang, L., Qiu, A., Kuai, B., Cong, P. & Guo, N. (2005). Study of the gas-puff line mass and density from Laval nozzle. *Hi. Power Laser Part. Beams* **17**, 295–298.

Whitney, K.G., Thornhill, J.W., Apruzese, J.P. & Davis, J. (1990). Basic considerations for scaling Z-pinch X-ray emission with atomic number. *J. Appl. Phys.* **67**, 1725–1735.

Zou, R., Liu, R., Zeng, N., Han, M., Yuan, J., Wang, X. & Zhang, G. (2006). A pulsed power generator for X-pinch experiments. *Laser Part. Beams* **24**, 503–509.

https://doi.org/10.1017/S0263034609990279 Published online by Cambridge University Press